PLASMA DYNAMICS

VIII. PLASMA PHYSICS*

Academic and Research Staff

Prof. G. Bekefi
Prof. W. P. Allis
Prof. S. C. Brown
Prof. J. C. Ingraham
Prof. B. L. Wright
Dr. W. M. Manheimer
J. J. McCarthy
W. J. Mulligan

Graduate Students

M. L. Andrews
A. J. Cohen
D. L. Flannery
E. V. George
P. W. Jameson
R. L. Kronquist
L. D. Pleasance
G. L. Rogoff
J. K. Silk
D. W. Swain
J. H. Vellenga

A RADIOFREQUENCY ABSORPTION IN PLASMAS

The interaction of RF fields with magneto-active plasma columns has been under investigation in this laboratory for several years.[1-5] The basic features of the experimental systems used in these experiments are shown in Fig. VIII-1. A coil is constructed to produce an axially periodic solenoidal RF field. The plasma interaction with this field results in a change in the impedance of the coil. The conservative field associated with any realizable coil structure is prevented from interacting with the plasma by an electrostatic shield.

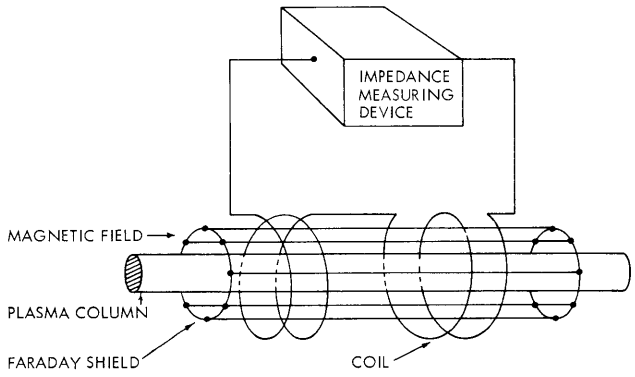

Fig. VIII-1.
General configuration of the RF coupling experiment.

In principle, the measured impedance can be related to the plasma properties through a self-consistent solution for the RF fields over all space. In practice, this is generally a rather difficult calculation. It has been shown, however, that, under certain circumstances, to a first approximation the fields in the plasma column may be taken to be the solenoidal field of the coil in the absence of plasma. Near ion cyclotron resonance, this requires that

*This work was supported principally by the U. S. Atomic Energy Commission (Contract AT(30-1)-1842).

$$\frac{\omega_{pi}^2}{2k^2c^2\Gamma} \ll 1, \tag{1}$$

where ω_{pi} is the ion plasma frequency, k is the dominant axial wave number of the RF field, and Γ is the half-width of the ion cyclotron absorption line. Equation 1 generally requires that the electron density be less than 10^{12}/cc in hydrogen. Equation 1 also represents the condition that ion cyclotron waves be strongly damped. This means that the measured conductance represents power absorption over the region of the plasma where the unperturbed RF fields from the coil are present, and does not represent power loss through wave propagation away from the coil.

The experiment now in progress involves experimental and theoretical examination of the effect of plasma thermal motion on coupling near ion cyclotron frequency. Broadening arising from ion-neutral collisions in helium has been examined previously by Glenn.[2,3] In a collisionless plasma with cold electrons, the ion cyclotron resonance absorption line will be broadened by ion thermal motion with a half-width kv_t, where $v_t = \sqrt{\frac{kT_i}{M_i}}$ is the ion thermal velocity. Recent measurements by Jameson have shown that electron thermal motion also contributes to broadening of the line.[4,5]

A double-ended hot-cathode PIG discharge has been constructed to determine the difficulties of operation at the low neutral pressures needed to insure that Doppler broadening be dominant ($p < 1$ μ in hydrogen). Figure VIII-2 shows a typical absorption curve obtained from this discharge as the DC magnetic field is swept slowly through ion cyclotron resonance. Detailed analysis requires addition of more plasma diagnostics

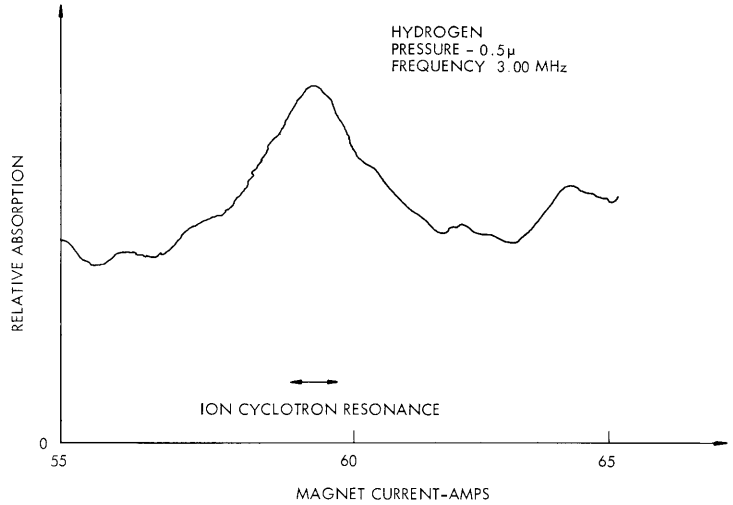

Fig. VIII-2. Relative absorption vs magnet current.

to the discharge.

The origin of the high off-resonant absorption (background) in Fig. VIII-2 is also under investigation. Similar effects have previously been attributed to direct coupling of the conservative field of the coil to the electrons of the plasma.[1] The electrostatic shield is designed to reduce this coupling. There is a possibility, however, that part or all of the background in Fig. VIII-2 is due to longitudinal charge separation set up in the plasma by the transverse fields. The usual approximation that the high mobility of electrons along the DC magnetic field lines results in charge neutrality is not valid in the low-pressure discharge used here. A numerical solution of the coupling problem is now being attempted to examine the effect of finite longitudinal electron mobility on absorption.

The impedance changes attributable to the plasma are much smaller than the impedance of the coil. The major technical problem encountered has been the development of detection systems capable of measuring the small impedance changes caused by the plasma. A marginal oscillator is being used, at present. This detection system combines simplicity of construction and operation with high sensitivity. A diagram of the basic system is shown in Fig. VIII-3. The coupling coil is the tank circuit of a low-level oscillator. The steady-state amplitude of the radiofrequency is controlled and

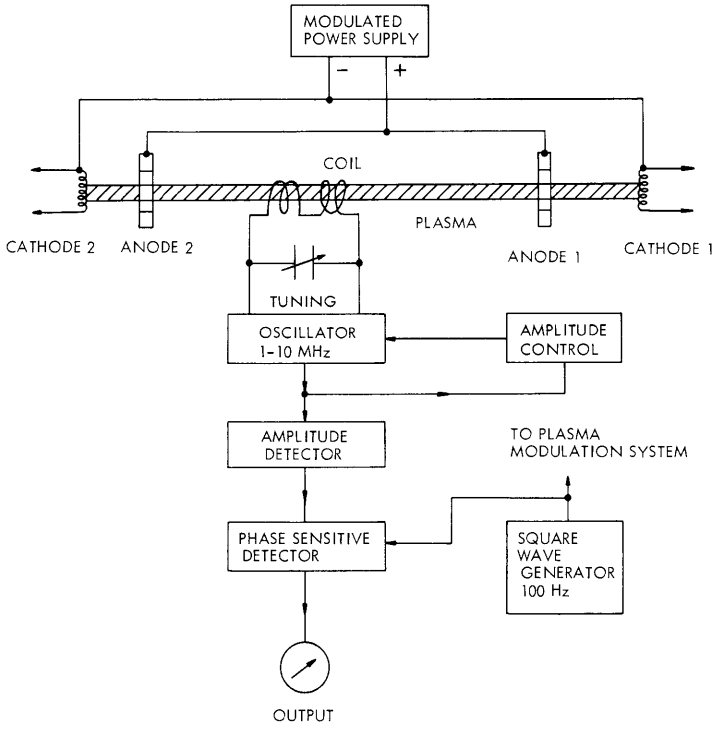

Fig. VIII-3. Detection system.

maintained by a suitable feedback system. If the plasma is modulated at a frequency higher than the response time of the amplitude control, the instantaneous RF amplitude is determined by the power lost in the plasma. If this RF signal is placed through an amplitude detector and the magnitude of the component at the modulation frequency examined, a signal proportional to the plasma absorption is obtained. Similarly, the steady-state frequency is determined by the coil admittance. The instantaneous frequency is determined by the dispersive properties of the plasma and may be detected with an FM receiver.

L. D. Pleasance

References

1. D. R. Whitehouse and P. J. Freyheit, Quarterly Progress Report No. 66, Research Laboratory of Electronics, M.I.T., July 15, 1967, pp. 98-100.
2. W. H. Glenn, Quarterly Progress Report No. 74, Research Laboratory of Electronics, M.I.T., July 15, 1964, pp. 69-73.
3. W. H. Glenn, Ph.D. Thesis, Department of Physics, M.I.T., 1966.
4. P. W. Jameson, Quarterly Progress Report No. 86, Research Laboratory of Electronics, M.I.T., July 15, 1967, pp. 123-128.
5. P. W. Jameson, Ph.D. Thesis, Department of Electrical Engineering, M.I.T., 1967.

B. BREMSSTRAHLUNG FROM A HIGHLY TURBULENT PLASMA AT HARMONICS OF THE PLASMA FREQUENCY

1. Introduction

It is well known[1,2] that a turbulent infinite plasma in zero magnetic field will radiate large-amplitude electromagnetic waves through Bremsstrahlung at the plasma frequency ω_p and at $2\omega_p$. If the plasma is highly turbulent, one would expect emission not only at these two frequencies, but also at all harmonics of the plasma frequency. A simple method is presented here for calculating the Bremsstrahlung at any harmonic of ω_p other than the fundamental, in terms of the turbulent spectrum.

Basically, a plasma emits radiation at $2\omega_p$ because a longitudinal wave at frequency (ω_p, k) accelerates particles at frequency ω_p, thereby causing the emission of transverse waves. Then if the density of radiating particles oscillates at (ω_p, k'), these two effects will couple to produce a transverse wave at $(2\omega_p, k+k')$. This is the familiar nonlinear process of resonant mode coupling. Now, since the plasma is a nonlinear medium, longitudinal electric fields at ω_p will drive both longitudinal electric fields and density fluctuations at all harmonics of ω_p. These driven fields and density fluctuations can also couple to produce transverse waves. They will be at various harmonics of the plasma frequency. We shall derive a general formula for Bremsstrahlung at any frequency.

We shall also work out the contributions for $\omega \approx 2\omega_p$ and $\omega \approx 3\omega_p$, and discuss the results.

2. General Expression for the Bremsstrahlung at Any Frequency

We start with the general expression for radiation from an accelerated charge at large distance,

$$E_{rad} = \frac{e}{c^2} \frac{x \times (x \times \dot{v})}{|x|^3}. \tag{1}$$

Equation 1 is the correct nonrelativistic expression, where E_{rad} is the amplitude of the transverse electromagnetic wave. Let us assume that the plasma is localized as in Fig. VIII-4, having total volume V, and the observer is much farther away than the dimensions of the plasma. The vector from the center of the plasma to the observer is x, and the acceleration $\dot{v}$ is evaluated at the retarded time

$$t' = t - \frac{|x-x'|}{c} = t - \frac{|x|}{c} + \frac{\hat{n} \cdot x'}{c}, \tag{2}$$

where $\hat{n}$ is the unit vector in the direction x, and x' is the position of the radiating electron with respect to an origin in the plasma.

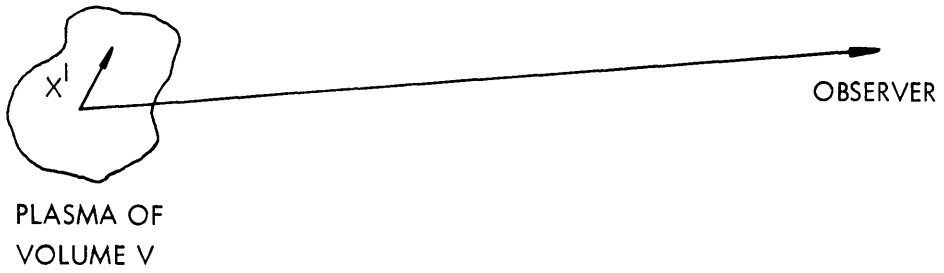

Fig. VIII-4. Plasma location with respect to the observer.

Let us say that the force on a particle comes from an electric field E caused by longitudinal plasma waves.

$$\dot{v} = \frac{e}{m} E(x, t). \tag{3}$$

Let the density of electrons be n(x, t). Then the radiation field of all electrons is

$$E_{rad} = \frac{e^2}{mc^2} \int d^3x' \; n(x', t') \frac{\vec{x} \times (\vec{x} \times E(x', t'))}{|x|^3}. \tag{4}$$

Now let us assume that n and E can be Fourier-transformed in space and time as

$$n(x',t') = \sum_{k\Omega} n_1(k,\Omega)\exp[i(kx'-\Omega t)] + \sum_{kk'\Omega\Omega'} n_2(kk'\Omega\Omega')\exp\{i[(k+k')x'-(\Omega+\Omega')t']\} + \ldots$$

$$+ \sum_{\substack{k_1\ldots k_r \\ \Omega_1\ldots\Omega_r}} n_r(k_1\ldots k_r,\Omega_1\ldots\Omega_r)\exp\{i[(k_1+\ldots+k_r)x'-(\Omega_1+\ldots+\Omega_r)t']\} + \ldots \tag{5}$$

$$E(x',t') = \sum_{k,\Omega} \mathscr{E}_1(k\Omega)\exp[i(kx'-\Omega t')] + \sum_{kk'\Omega\Omega'} \mathscr{E}_2(kk'\Omega\Omega')\exp\{i[(k+k')x'-(\Omega+\Omega')t']\}$$

$$+ \sum_{\substack{k_1\ldots k_r \\ \Omega_1\ldots\Omega_r}} \mathscr{E}_r(k_1\ldots k_r,\Omega_1\ldots\Omega_r)\exp\{i[(k_1+\ldots+k_r)x'-(\Omega_1+\ldots+\Omega_r)t']\} + \ldots \tag{6}$$

In general, the waves E_1 satisfy the linear theory, while the $E_{r>1}$ are driven fields set up by the nonlinear interactions of the plasma with the E_1's. Since the turbulent fluctuations in the plasma are assumed to be electrostatic,

$$n_r = \frac{(\vec{k}_1+\ldots+\vec{k}_r)\cdot\vec{\mathscr{E}}_r}{4\pi e}. \tag{7}$$

Inserting expressions (5), (6), and (7) in (4) yields

$$E_{rad} = \sum_{rs}\frac{e^2}{mc^2}\int d^3x' \sum_{\substack{k_1\ldots k_{r+s} \\ \Omega_1\ldots\Omega_{r+s}}} \frac{\hat{n}\times[n\times\mathscr{E}_r(k_1\ldots k_r,\Omega_1\ldots\Omega_r)]}{x}$$

$$\cdot\frac{(\vec{k}_{r+1}\ldots\vec{k}_{r+s})\cdot\mathscr{E}_s(k_{r+1}\ldots k_{r+s},\Omega_{r+1}\ldots\Omega_{r+s})}{4\pi e}\exp\left\{i\left[\sum_{i=1}^{r+s}k_i\cdot x' - \sum_{i=1}^{r+s}\Omega_i t'\right]\right\}. \tag{8}$$

Introducing retarded time in Eq. 8 and performing the integral over all space yields

$$E_{rad} = \sum_{rs} \frac{e^2}{mc^2} \sum_{\substack{k_1 \cdots k_{r+s} \\ \Omega_1 \cdots \Omega_{r+s}}} V \frac{\hat{n} \times [n \times \vec{\mathscr{E}}_r(k_1 \cdots k_r, \Omega_1 \cdots \Omega_r)]}{x} [\vec{k}_{r+1} + \cdots + \vec{k}_{r+s}]$$

$$\cdot \frac{\vec{\mathscr{E}}_s(k_{r+1} \cdots k_{r+s}, \Omega_{r+1} \cdots \Omega_{r+s})}{4\pi e} \delta \left[\sum_{i=1}^{r+s} \left(\vec{k}_i - \frac{\Omega_i \hat{n}}{c} \right) \right] \exp \left\{ -i \left[\sum_{i=1}^{r+s} \Omega_i \left(t - \frac{x}{c} \right) \right] \right\}, \tag{9}$$

where the Kroneker delta function, δ, is 1 when its argument is zero and zero otherwise. It simply means that the wave numbers of all plasma waves add to give the wave number of the transverse wave. The terms in Eq. 9 are simply spherical electromagnetic waves of frequency $\Omega_1 + \ldots + \Omega_{r+s}$ and of velocity c. The amplitude of the electric field at each frequency is given by the coefficient of the oscillatory term. Let us note that since the observer at x is taken to be outside the plasma, the wave is treated as an electromagnetic wave in free space having velocity c. This wave is actually formed inside the plasma, however, and if (9) is to be valid, it must be able to freely propagate out. That is, the wave's dispersion relation must be roughly the same inside the plasma and outside. Thus, (9) is approximately correct for $\omega \approx n\omega_p$, $n > 1$, where the plasma is almost transparent. It would not be at all accurate at $\omega \leq \omega_p$ where the propagation differs radically, the difference depending upon whether one is inside or outside the plasma.

If the amplitude of an electromagnetic wave at frequency ω is $E(\omega)$, the quantity of interest is usually the intensity $I(\omega) = \left\langle |E(\omega)|^2 \right\rangle$ or power spectrum. The ensemble average is taken over the random phases of the waves. Thus, if $\sum_{i=1}^{r+s} \Omega_i$ in Eq. 9 is defined as ω,

$$I(\omega) = \left\langle \left| \frac{e}{mc^2} \sum_{rs} \sum_{\substack{k_1 \cdots k_{r+s} \\ \Omega_1 \cdots \Omega_{r+s}}} V \frac{\hat{n} \times [\hat{n} \times \vec{\mathscr{E}}_r(k_1 \cdots k_r, \Omega_i \cdots \Omega_r)]}{x} (\vec{k}_{r+1} + \cdots \vec{k}_{r+s}) \right. \right.$$

$$\left. \left. \cdot \frac{\vec{\mathscr{E}}_s(k_{r+1} \cdots k_{r+s}, \Omega_{r+1} \cdots \Omega_{r+s})}{4\pi e} \delta \left[\sum_{i=1}^{r+s} \vec{k}_i - \vec{K} \right] \right|^2 \right\rangle, \tag{10}$$

where $\sum_{i=1}^{r+s} \frac{\Omega_i \hat{n}}{c} = \vec{K}$, the wave number of the transverse wave. Thus, the problem reduces to finding the E_r's. Generally the E_r's are calculated by an iterative procedure. That is, let us say that the plasma supports turbulent fluctuations of the form

$$E(x,t) = \sum_k \vec{\mathscr{E}}_k \exp[i(k\cdot x - \omega t + \phi_k)] \qquad \text{or} \qquad \vec{\mathscr{E}}(k,\Omega) = \vec{\mathscr{E}}_k \delta[\Omega - \omega_k]$$

$$\delta[\Omega - \omega_k] = 1 \qquad \Omega = \omega_k$$

$$\delta[\Omega - \omega_k] = 0 \qquad \Omega \neq \omega_k \tag{11}$$

which can be described adequately in the linear theory. That is, $\omega = \omega_k$, the value given by the linear dispersion relation. We also assume

$$\frac{\sum_k |\vec{\mathscr{E}}_k|^2}{nmV_T^2} \ll 1,$$

or the turbulent fluctuation energy is much less than the total particle thermal energy; and $\omega/k \gg V_T$, or there are no particles that are resonant with the wave. We also assume that the phases ϕ_K are random. Then, since the plasma is a nonlinear medium, the waves of (11) will drive other waves of the form

$$\vec{\mathscr{E}}_n(x,t) = \sum_{k_1 \ldots k_n} \vec{\mathscr{E}}_n(k_1 \ldots k_n) \exp\{i[(\vec{k}_1 + \ldots + \vec{k}_n)\cdot \vec{x}' - (\omega_1 + \ldots + \omega_n)t]\}. \tag{12}$$

The amplitude E_n will go roughly as

$$\vec{\mathscr{E}}_1 \left[\frac{\sum_k |\vec{\mathscr{E}}_k|^2}{nmV_T^2}\right]^{\frac{n-1}{2}}$$

Several other comments can be made about the driven fields. First, since a plasma can support electrostatic oscillations only at roughly the plasma frequency, the $E_{n>1}$ of Eq. 12 cannot be natural modes of oscillation of the medium because $\omega_n \approx n\omega_p$. There can be no parametric growth of these waves. Also, the random phase of the wave E_n is simply $\phi_{K1} + \ldots + \phi_{Kn}$, the sum of the phases of the waves at $k_1 \ldots k_n$ which drive the system. Thus, the phases of the individual Fourier components of $E_{r>1}$ are not random with respect to one another. The phases of the $E_1(k,\omega)$ are random, however. Finally, let us note that since $\omega/k \gg V_T$, $\frac{\omega_1 + \ldots + \omega_n}{k_1 + \ldots + k_n} \gg V_T$ also for any n. Thus, the particles are not resonant with any part of the turbulent wave spectrum, fundamental or driven harmonics.

We should also note that since the turbulent fields must be purely real, $\phi_K = -\phi_{-K}$ and $\vec{\mathscr{E}}_r(k_1 \ldots k_r) = \vec{\mathscr{E}}_r^*(-k_1 \ldots k_r)$. The procedure now is to assume some turbulent

spectrum in the plasma of the form (11) and use an iterative procedure as outlined, for instance, by Drummond and Pines[3] to obtain the $\vec{\mathscr{E}}_r$. Thus, the Bremsstrahlung will be in terms of the amplitudes of the turbulent spectrum.

3. Calculation at $\omega \approx 2\omega_p$

Since $E_{K=0} = 0$, the only term in Eq. 10 that gives a contribution at $\omega = 2\omega_p$ is the $r = s = 1$ term. Let us define $\vec{\mathscr{E}}_1 = \hat{k}\vec{\mathscr{E}}_1$, where k is a unit vector in the direction of $\vec{k}$ (and also $\vec{E}_K$). Then (10) becomes

$$I(\omega) = \left\langle \left(\frac{e}{4\pi mc^2}\right)^2 \left| \sum_k \frac{\hat{n}\times(\hat{n}\times\hat{k})}{x} \vec{\mathscr{E}}_k |\vec{K}-\vec{k}|\, \vec{\mathscr{E}}_{K-k} V \right|^2 \right\rangle, \tag{13}$$

where $\omega = \omega_k + \omega_{K-k}$, and $\vec{K} = \frac{\omega}{c}\hat{n}$, the free space wave vector. Symmetrizing yields

$$I(\omega) = \left\langle \frac{1}{4}\left(\frac{e}{4\pi mc^2}\right)^2 V^2 \left| \sum_k \frac{\hat{n}\times(\hat{n}\times\hat{k})}{x} \vec{\mathscr{E}}_k |K-k|\, \vec{\mathscr{E}}_{K-k} + \frac{\hat{n}\times(n\times\widehat{K-k})}{x} \vec{\mathscr{E}}_k |k|\, \vec{\mathscr{E}}_{K-k} \right|^2 \right\rangle. \tag{14}$$

Now, since $k \gg K$, to first order in K/k,

$$\widehat{K-k} = -\hat{k} + \frac{\vec{K}}{|k|} - \frac{\vec{k}\, k\cdot K}{k^3}, \qquad |K-k| = k - \frac{k\cdot K}{k}. \tag{15}$$

Then, by combining terms, (14) becomes

$$I(\omega) = \left(\frac{e}{4\pi mc^2}\right)^2 V \left| \sum_k \frac{n\times(n\times\hat{k})}{x} \frac{k\cdot K}{k} \vec{\mathscr{E}}_k \vec{\mathscr{E}}_{K-k} \right|^2. \tag{16}$$

Writing out the square of the brackets in the parentheses yields a double summation, over k and k'. A term will immediately ensemble-average to zero unless $k = -k'$, or $k = k' - K$ when the ensemble average over phase simply gives unity. Thus, ensemble averaging gives

$$I(\omega) = \left(\frac{eV}{4\pi mc^2}\right)^2 \frac{1}{x^2} \sum_k [\hat{n}\times(\hat{n}\times\hat{k})]^2 \left[\frac{k\cdot K}{k}\right]^2 |\vec{\mathscr{E}}_k|^2\, |\vec{\mathscr{E}}_{K-k}|^2. \tag{17}$$

We see that the result has a factor of K^2/k^2, as is known to be the case for Bremsstrahlung at $\omega \approx 2\omega_p$.

4. Calculation at $\omega \approx 3\omega_p$

For $\omega \approx 3\omega_p$, there are two possibilities in Eq. 10, r = 1, s = 2, and s = 1, r = 2. Then (10) becomes

$$I(\omega) = \left\langle \left(\frac{eV}{4\pi mc^2 x}\right)^2 \left| \sum_{kk'} \hat{n}\times(\hat{n}\times\widehat{K-k-k'})\, \mathcal{E}_{K-k-k'} \left|k+k'\right| \mathcal{E}_{k+k'} \right.\right.$$
$$\left.\left. + \hat{n}\times(\hat{n}\times\widehat{k+k'})\, \mathcal{E}_{k+k'} \left|K-k-k'\right| \mathcal{E}_{K-k-k'} \right|^2 \right\rangle, \tag{18}$$

where $\omega = \omega_k + \omega_{k'} + \omega_{K-k-k'}$, and $\vec{K} = \frac{\omega_k + \omega_{k'} + \omega_{K-k-k'}}{c}\hat{n}$, the free-space wave number. Then, upon making the same expansion as before, (18) becomes

$$I(\omega) = \left(\frac{e}{4\pi mc^2}\right)^2 \frac{V^2}{x^2} \left| \sum_{kk'} n\times(n\times\widehat{k+k'}) \frac{(\overrightarrow{k+k'})\cdot\vec{K}}{\left|k+k'\right|} \mathcal{E}_{k+k'} \mathcal{E}_{K-k+k'} \right|^2 . \tag{19}$$

Before we can proceed, we must calculate $E_{k+k'}$. Drummond and Pines[3] have shown how to calculate it by the use of an iteration scheme resembling the Born approximation. Their result is

$$\vec{\mathcal{E}}_{k+k'} = \frac{-\omega_p^2(\overrightarrow{k+k'})\frac{e}{m}}{\epsilon(k+k',\omega+\omega')\left|k+k'\right|^2} \mathcal{E}_k \mathcal{E}_{k'} \hat{k}_j \hat{k}'_\ell \int_c \frac{dv}{(\omega+\omega') - (k+k')\cdot v} \frac{\partial}{\partial v_j} \frac{1}{\omega' - k'\cdot v} \frac{\partial}{\partial v_\ell} f, \tag{20}$$

where c refers to the Landau contour of integration, and $\epsilon(k+k',\omega+\omega')$ refers to the dielectric constant of the plasma,

$$\epsilon(k+k',\omega+\omega') = 1 - \frac{\omega_p^2}{(\omega+\omega')^2} \approx \frac{3}{4}. \tag{21}$$

The integral of (20) can be evaluated with a moment expansion of the denominators to yield

$$\vec{\mathcal{E}}_{k+k'} = \frac{-2\omega_p^2(\overrightarrow{k+k'})\frac{e}{m}}{3\left|k+k'\right|^2} \mathcal{E}_k \mathcal{E}_{k'} \left[\frac{kk' + k'^2\cos\theta}{(\omega+\omega')^2\omega'^2} + \frac{kk' + k^2\cos\theta}{(\omega+\omega')^2\omega^2} + \frac{2(k^2+k'^2)\cos\theta + 2kk'(1+\cos^2\theta)}{(\omega+\omega')^3\omega'} \right.$$
$$\left. + \frac{2(k+k')^2\cos\theta + 2kk'(1+\cos^2\theta)}{(\omega+\omega')^3\omega} \right],$$

where the result has been symmetrized with respect to exchanging k and k', and θ is the angle between $\vec{k}$ and $\vec{k}'$, that is, $\cos\theta = \hat{k}\hat{k}'$. Thus the summand of (19) is symmetric with respect to exchanging k and k'. Making use of the random phase approximation, (19) becomes

$$I(\omega) = 6\left(\frac{e^2}{4\pi m^2 c^2}\right)^2 \frac{V^2}{x^2} \sum_{kk'} [n\times(n\times\widehat{k+k'})]^2 \left[\frac{(\vec{k+k'})\cdot\vec{K}}{|k+k'|}\right]^2 |\mathscr{E}_k|^2 |\mathscr{E}_{k'}|^2 |\mathscr{E}_{k-k'}|^2$$

$$\cdot \frac{4\omega_p^2}{9|k+k'|^2}\left\{\frac{kk'+k'^2\cos\theta}{(\omega+\omega')^2\omega'^2} + \frac{kk'+k'^2\cos\theta}{(\omega+\omega')^2\omega^2} + 2\frac{(k^2+k'^2)\cos\theta + kk'(1+\cos^2\theta)}{(\omega+\omega')^3\omega}\right.$$

$$\left. + 2\frac{(k^2+k'^2)\cos\theta + kk'(1+\cos^2\theta)}{(\omega+\omega')^3\omega'}\right\}^2 \qquad (22)$$

Comparing Eq. 17 with Eq. 22, we can see that the intensity at $\omega \approx 3\omega_p$ is down roughly by a factor of

$$\frac{\sum_K |\mathscr{E}_K|^2}{nm\left(\frac{\omega_p}{k}\right)^2} = \frac{\text{wave energy}}{\text{thermal energy}} \times \left(\frac{\text{thermal velocity}}{\text{phase velocity of turbulent waves}}\right)^2 \qquad (23)$$

from the intensity at $\omega \approx 2\omega_p$.

Thus, we see that the contribution to the Bremsstrahlung at $\omega \approx 3\omega_p$ is quite small, as compared with the contribution at $2\omega_p$.

5. Discussion

We have calculated the Bremsstrahlung at $2\omega_p$ and $3\omega_p$ from a highly turbulent plasma. It is clear that unless the turbulence is quite strong, the contribution at $3\omega_p$ is very weak. There is one point that should be made concerning the validity of a nonrelativistic calculation. Relativistically, a charge oscillating at frequency ω radiates energy not only at ω, but also at all harmonics of ω, the intensity of the n+1 at harmonic being down by roughly a factor of $\left(\frac{v}{c}\right)^2$ from the n^{th}. Thus, if the plasma is relativistic, or if

$$\left(\frac{v_T}{c}\right)^2 > \frac{\text{wave energy}}{\text{thermal energy}}\left(\frac{\text{thermal velocity}}{\text{wave phase velocity}}\right)^2,$$

relativistic effects must be included.

W. M. Manheimer

References

1. T. Birmingham, J. Dawson, and C. Oberman, Phys. Fluids 8, 297 (1965).
2. D. A. Tidman and T. H. Dupree, Phys. Fluids 8, 1860 (1965).
3. W. Drummond and D. Pines, Nucl. Fusion Suppl. 1049 (1962).

C. DIFFUSION WAVE EXPERIMENT

A basic change has occurred in the nature of this experiment, previously described in Quarterly Progress Report No. 82 (pages 97-98). The present approach is to excite one-dimensional radial diffusion waves, rather than two-dimensional longitudinal-radial waves. One reason for the change is that longitudinal plasma transport is more appropriately characterized as free-streaming rather than as diffusion, at these low pressures (~10^{-3} Torr). Thus we have the limit of the two-dimensional diffusion waves in which $D_{||}$ approaches infinity, that is, radial diffusion dominates. A second reason for the change is the difficulty involved in producing a modulated plasma source at the cathode, as compared with the simple method of modulating arc current. The latter method causes plasma density modulation in the arc column, which is then a cylindrical plasma source for the surrounding plasma.

1. D-C Arc

The DC arc properties and arc geometry play an important role in determining diffusion wave properties and will be briefly discussed. The essential geometric features are shown in Fig. VIII-5. Although the electrodes are somewhat removed from the glass tube, they are expected to determine the end conditions of the plasma, because of the connecting magnetic field lines along which the plasma may stream freely. To promote uniform end conditions it would be desirable to have end plates that are somewhat larger in diameter than the glass tube. This configuration was tried and would not allow stable arc operation with parameters of interest. Therefore the present configuration, with smaller anode, was settled upon. With this configuration the arc runs stably with the following parameters.

Cathode flow (Argon):	1.2 atm-cm^3/sec
Ambient pressure:	approx. 10^{-3} Torr
Arc current:	5.5 amps
Arc voltage:	40-50 volts
Magnetic field:	200-1000 Gauss.

The presence of instabilities is indicated by noise on the arc current and Langmuir probe current, as a function of magnetic field. There is a relatively quiet region at approximately 600 Gauss. For excursions either up or down in magnetic field,

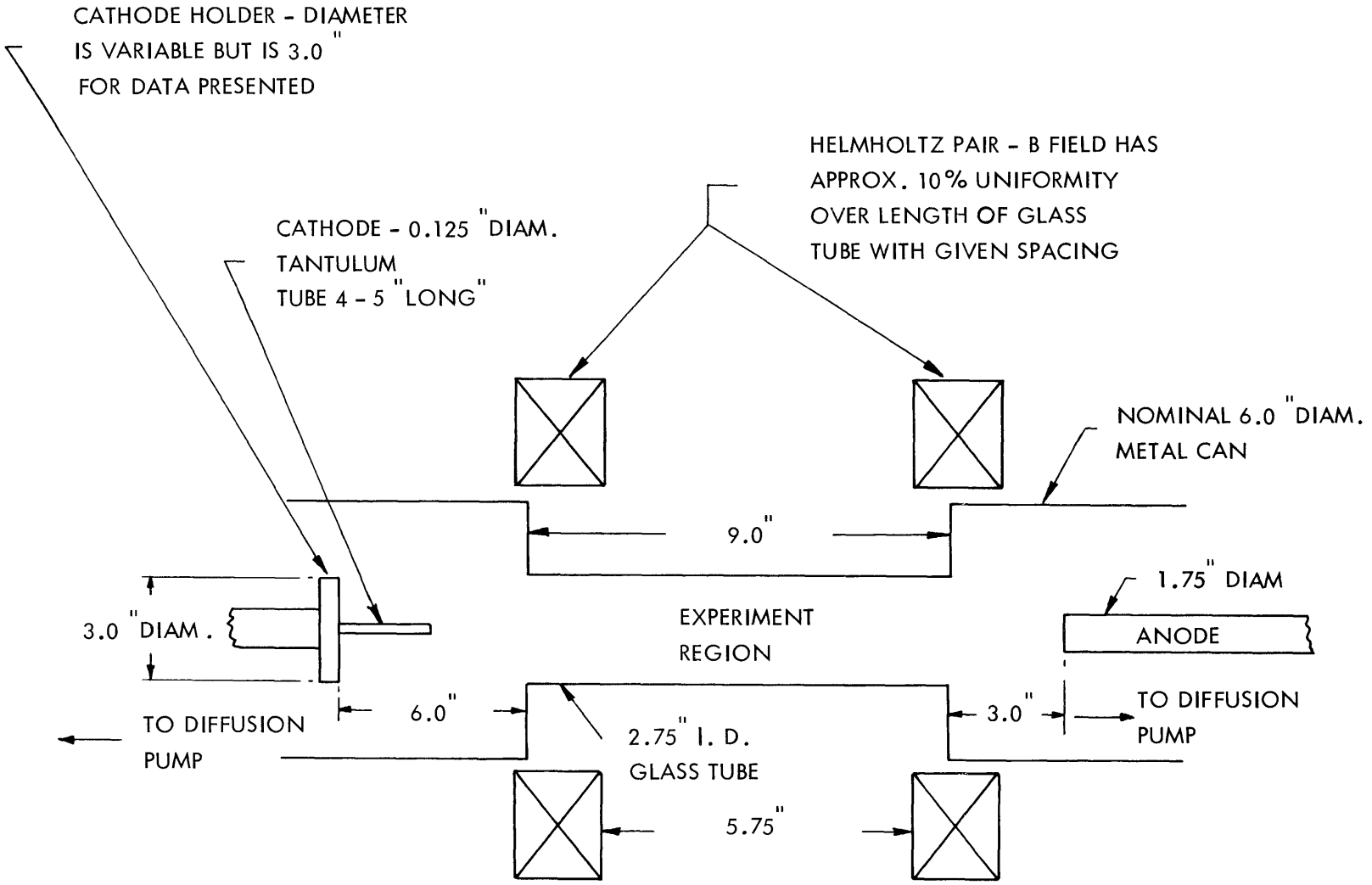

Fig. VIII-5. Arc geometry.

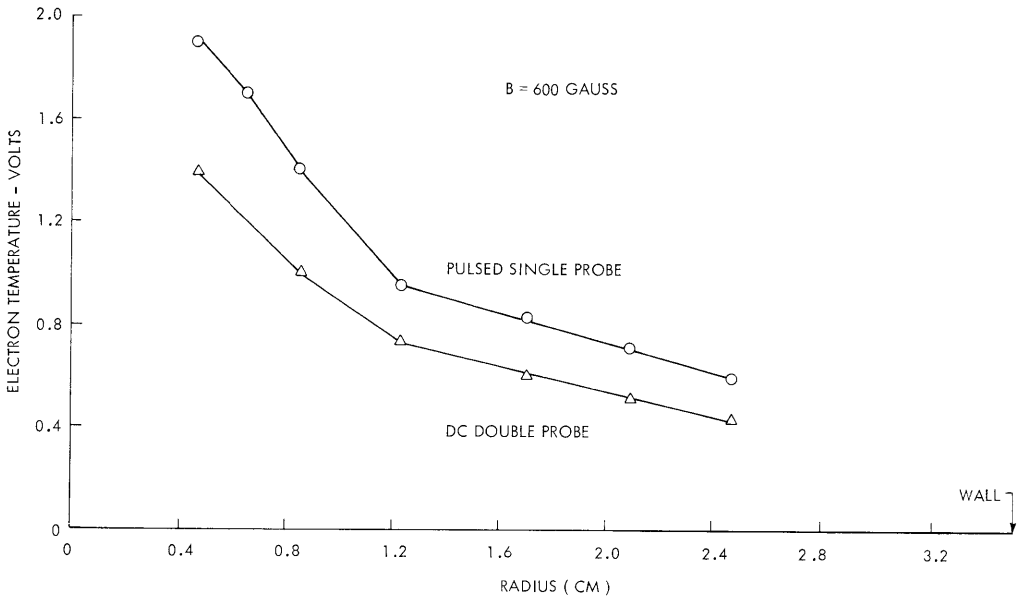

Fig. VIII-6. Electron temperature profiles from pulsed and double probes.

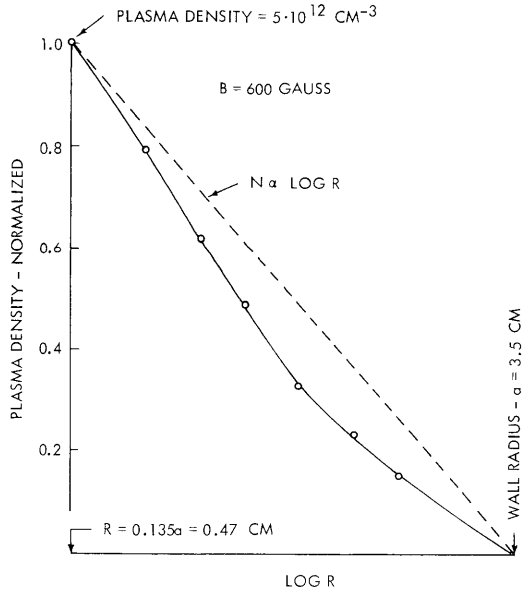

Fig. VIII-7. DC plasma density profile.

narrow-band noise appears at several kilocycles, and rapidly becomes wide-band for larger excursions. The waveform of the narrow-band noise is different at the lower magnetic fields than at the higher values. The rms noise level on the arc current is ~10-20 mA in the quiet zone, or ~0.2-0.4%. These instabilites have not been investigated extensively but are suggestive of those predicted theoretically by Woo[1] for low-pressure arcs of this type.

The DC plasma appears to be a thin column; however, Langmuir probe studies show that the invisible surrounding plasma is of the same order of magnitude in plasma density as the central visible column. The visible column cannot be studied with stationary probes (because of heating); however, moving Langmuir probe diagnostics have established plasma densities of $\sim 10^{13}$ cm^{-3} and temperatures of 3-4 volts. Figures VIII-6 and VIII-7 are plasma density and electron temperature profiles for the DC arc, starting from ~0.5 cm radius. A movable flat double probe is used, which can also be used as a single probe with coaxial shield. The probe surfaces face across the magnetic field. The electron temperature was obtained by using standard methods from both pulsed single-probe and static double-probe characteristics. The results are plotted in Fig. VIII-6, and the pulsed-probe values are consistently ~35% higher. Both methods yield the same profile shape, which is more important in the theory.

The plasma density profile shown in Fig. VIII-8 was calculated from the ion saturation current and the pulsed-probe values of electron temperature. The measured density profile falls somewhat below the log (R) profile which corresponds to radial diffusion in a uniform plasma. This is probably due to such effects as end loss and temperature

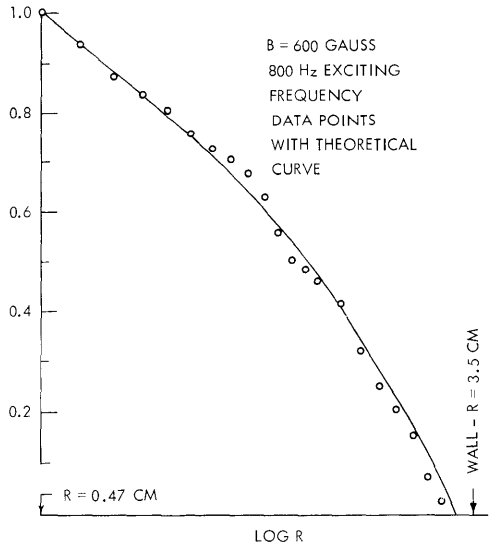

Fig. VIII-8. Diffusion wave amplitude profile at 800 Hz with theoretical curve.

gradients, which make this plasma less ideal. The anode radius also presents a change in end conditions that can possibly affect both plasma end losses, and also radial diffusion coefficients, through a Simon short-circuit effect.

2. Experimental Results

Arc current is modulated, and radial phase and magnitude profiles of the ion saturation current modulation to a Langmuir probe have been measured by using a phase-sensitive detector. Phase resolved pulsed-probe measurements indicate plasma density modulations of 5% or less at typical operating levels, while the corresponding electron temperature modulation was not detectable. Phase and amplitude changes along the magnetic field were measured and were negligible, as compared with radial variations, thereby lending credence to a one-dimensional model of radial diffusion waves. Signal-to-noise ratios were good and results repeatable.

The ion saturation current amplitude modulation was corrected by the square root of the measured electron temperature to yield plasma density modulation amplitude according to the Bohm formula: $J_{+S} \propto n\sqrt{T_e}$. Figures VIII-8 and VIII-9 show data points taken with the arc in its most quiet region of operation.

3. Theory

We start by assuming that two basic equations are applicable:

$$\nabla \cdot \Gamma + \frac{\partial n}{\partial t} = 0$$

$$\Gamma = -K \nabla(nT),$$

where Γ = "plasma" particle transport current, n = plasma density, and $T = T_+ + T_- \approx T_-$ (in volts). Some justification is called for in stating these equations, but it is beyond the scope of this report. Two cases are likely for K:

Classical Diffusion: $$K = K_c \frac{n}{B^2 (T_e)^{3/2}} \qquad \text{(highly ionized)}$$

Anomalous Bohm Diffusion: $K = K_B/B,$

where B is the magnetic field strength. Theoretical work thus far has treated only the simpler case of Bohm diffusion, in which the equations are linear in plasma density. Combining the two basic equations, we have

$$\frac{\partial \Gamma_z}{\partial z} - \nabla_\perp \cdot K_\perp \nabla_\perp (nT) + \frac{\partial n}{\partial t} = 0.$$

The $\partial \Gamma_z / \partial z$ term represents the end loss of plasma. If we make a crude approximation

that the plasma is uniform along the B field and integrate the equation over z, we obtain

$$\frac{\Gamma_z(+L/2) - \Gamma_z(-L/2)}{L} - \nabla_\perp \cdot K_\perp \nabla_\perp (nT) + \frac{\partial n}{\partial t} = 0.$$

Γ_z at $z = \pm L/2$ can be approximated by a sheath loss term at the ends.

$$\Gamma_z(\pm L/2) = \pm n V_{SHEATH} \cong \pm n \sqrt{\frac{e(T_+ + T_-)}{M_+}}.$$

V_{SHEATH} is an effective plasma loss velocity into the end sheaths. Substituting, we obtain

$$\frac{1}{r}\frac{\partial}{\partial r} K_\perp r \frac{\partial}{\partial r}(nT) = \frac{\partial n}{\partial t} + \frac{2nV_{SHEATH}}{L}.$$

Taking first-order perturbations, expanding and linearizing yield

$$\frac{1}{r}\frac{\partial}{\partial r} K_\perp r \frac{\partial}{\partial r}(n_1 T_o + n_o T_1) = \frac{\partial n_1}{\partial t} + \frac{2n_1 V_{SHEATH}}{L}.$$

A further assumption, verified by the previously mentioned pulsed probe studies, is

$$\frac{T_1}{T_o} \ll \frac{n_1}{n_o},$$

which allows us to drop the $(n_o T_1)$ term. With sinusoidal time dependence and the Bohm form of $K_\perp$ assumed, the final equation is

$$\frac{1}{r}\frac{\partial}{\partial r} r \frac{\partial}{\partial r}(n_1 T_o) = \left(\frac{i\omega}{K_\perp} + \frac{2V_{SHEATH}}{KL}\right) n_1.$$

This equation has been solved by a digital computer, using the facilities of Project MAC at M.I.T., subject to the boundary condition n = 0 at some (effective wall) radius. The measured T_o profile is approximated (in many cases by an exponential variation), by an analytic function that is used in the computer solution. To account for a possible end condition change at the anode radius, the plasma model has an inner and an outer region with a transition in between. The transition is made about an ion Larmor radius, approx. 1 cm thick, and is centered at the anode radius. The two regions are assumed to have generally different end-loss parameters ($2V_{SHEATH}/KL$), and different diffusion coefficients. A simple linear variation of these parameters through the transition layer was used. The effective wall radius is inferred from the data, and is usually somewhat less than the actual wall radius. (See Fig. VIII-8.) Thus, the computer solutions are matched to the data by choosing the correct set of 4 parameters (2 diffusion coefficients

and 2 end-loss parameters).

The smooth curves in Figs. VIII-8 and VIII-9 are the results of such computer fits to data sets for 400 Hz and 800 Hz modulating frequencies. The plasma is the one characterized by Figs. VIII-6 and VIII-7. The amplitude profile is plotted only for 800 Hz to avoid cluttering the graph, since the 400-Hz plot is very similar. For the 400 Hz case, 3 parameters were used, since the two end-loss values were taken as the same. In the

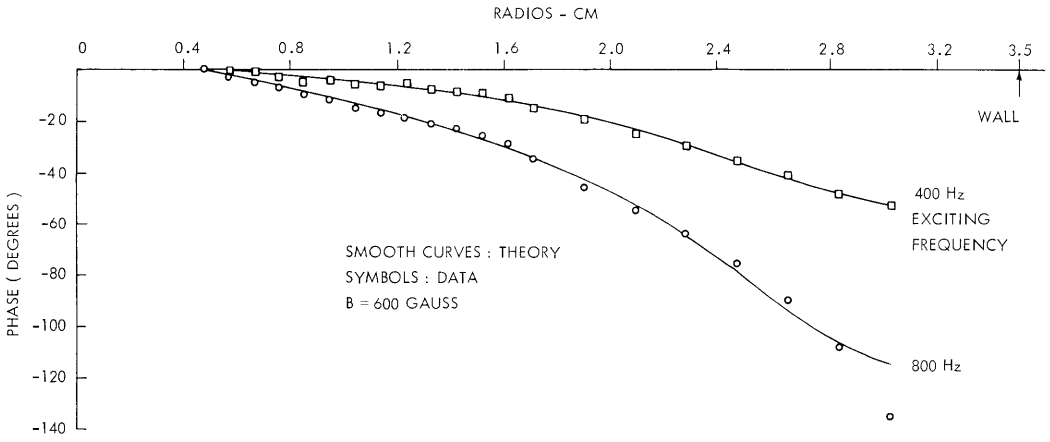

Fig. VIII-9. Diffusion wave phase profiles with theoretical curves.

800 Hz case the best fit was found for end-loss parameters of zero, so that only 2 parameters were used. It should be pointed out that the end-loss parameters affect mainly the amplitude profiles, and these are also affected strongly by the exact choice of T_o profile. Thus the value of end-loss parameter required for a fit may be related more to a small error in the T_o profile, than to actual end loss. Expected accuracy is less in the amplitude profile data than in the phase profile data, and errors there could affect the end-loss parameter required in a similar way. The T_o profile used was exponential with an e-folding length of 0.95 cm, which was a reasonable approximation to the profile of Fig. VIII-6.

If we take the fit parameters used at face value, they indicate the following diffusion coefficients

Modulating Frequency	Diffusion Coefficient (10^3 cm^2/sec)	
	Inner	Outer
400 Hz	26	1.1
800 Hz	18	1.1

The "inner" and "outer" values are for 0.5 cm and 2.4 cm radii, respectively. Because of the difference in T_e at the two points, the $D_\perp$ values would have a 3:1 inner-to-outer ratio, even if the diffusion mechanism is the same, since $D \propto T_e$. The corresponding theoretical values are the following.

	Theoretical $D_\perp$ (10^3 cm^2/sec)	
Theory	Inner	Outer (cm^2/sec)
Bohm	20	6.7
Classical	3.0	1.0

The "measured" values correspond much better to the Bohm figure in the inner region and to the classical value in the outer region. Thus the validity of the use of Bohm diffusion in the theory is questionable in the outer region. The end-loss parameter used in the 400 Hz case is physically reasonable, since it implies a sheath loss velocity of the same order of magnitude as the ion thermal velocity. The requirement of end loss, however, for a fit for only the lower frequency data is unphysical, and is more likely the result of inaccuracy in one of the measured amplitude profiles, or a basic fault in the theoretical model. The last possibility appears more likely, in view of recent attempts to explain data taken at higher magnetic fields (up to 1000 Gauss). These data seem to call for a model with a transition region at a radius much less than that of the anode, and we suspect that a classical (nonlinear) diffusion wave theory may be necessary.

If a suitable theory can be developed, the dependence of the diffusion coefficient on magnetic field, noise level of instabilities, and other parameters might be studied.

D. L. Flannery

References

1. J. C. Woo, Ph.D. Thesis, M.I.T., June 1966.